# Image Restoration in Optical-Sectioning Microscopy Using Projections onto Convex Sets

*M.R.P. Homem[1]; N.D.A. Mascarenhas[2] and L. da F. Costa[1]*

*[1] Instituto de Física de São Carlos, Universidade de São Paulo, USP - Av. Trabalhador São Carlense, 400, CEP:13.560-970, São Carlos, SP, Brazil; [2] Departamento de Computação, Universidade Federal de São Carlos, UFSCar - Via Washington Luís, Km 235, CP 676, CEP: 13.565-905, São Carlos, SP, Brazil.*

**Abstract**

We propose in this paper an approach to perform the deconvolution of three-dimensional biological images obtained by fluorescence microscopy based on the Projection onto Convex Sets that is an important result from vector-space projections theory. We suggest the use of three sets of convex constraints where the first one is to perform the three-dimensional deconvolution, the second set is to perform super-resolution (partially recovery of the missing cone of frequencies) and the last one is to guarantee the positiveness of the solution. Due to the presence of Poisson noise in the images acquired by fluorescence microscopes using CCD cameras, we propose Goodman and Belsher's filter, which considers this kind of noise, to be used in the first set. In order to use the filter in a POCS methodology, it is put in the form of a prototype image constraint. We have tested the algorithm using both synthetic and bead images and also with real cells images. The method was characterized by fast convergence rate and also demonstrated a good performance in terms of both visual results and cost-benefit analysis.

**Keywords:** 3D Deconvolution, COSM, POCS, Convex Sets, 3D Image Restoration, Poisson Noise.

## Introduction

This work presents an alternative iterative approach to perform the deconvolution of three-dimensional (3D) biological images [1] acquired by fluorescence microscopy based on the projection onto convex sets (POCS) theory [2]. Three-dimensional data are essential for the analysis of many structures of biological specimens and play an important role in biomedical research. For instance, the range of applications of 3D microscopic images extends from 3D visualization of a cell up to morphometry in neuroscience research. Particularly, in neuromorphology, defining the relationship between structure and function of neurons is important to further improve the understanding of the cells [3].

Commonly, computational optical sectioning microscopy (COSM) techniques are used to obtain a 3D data volume of biological specimens [4] where the image is formed by stacking a series of two-dimensional (2D) images that are acquired by using fluorescence microscopy [5][6]. We can find different forms of fluorescence microscopy (light microscopy), including confocal, deconvolution microscopy, where the images are acquired with a conventional wide-field fluorescence microscope, and two-photon microscopy. Both confocal and wide-field microscopes produce images with poor lateral and axial resolution although the confocal one exhibits an improved axial resolution as compared with wide-field microscope. For this reason, deconvolution algorithms can also be applied to confocal images to further improve the resolution, but for most practical purposes these are already satisfactory. On the other hand, the deconvolution microscope has some advantages over the confocal microscope as, for instance, the capability to work with wavelengths not provided by standard lasers.

In COSM a 3D image is a set of 2D images (optical slices), which are acquired by moving the microscope focus along the optical axis (axial direction). This technique of optical slicing has the disadvantage that each slice is obstructed (blurred) by out-of-focus information, which affects each image from adjacent slices. The mechanism of degradation (blurring) can be described by modeling the microscope's optics and also the detection process.

Mathematically, the observed 3D image $b(x, y, z)$ in the absence of any kind of noise is given by

$$b(x,y,z) = h(x,y,z) * f(x,y,z) \quad (1)$$

where $f(x,y,z)$ is the specimen function, $h(x,y,z)$ is the point spread function (PSF) of the microscope and * means 3D convolution. In the Fourier domain the problem becomes

$$B(u,v,w) = H(u,v,w) \cdot F(u,v,w) \quad (2)$$

where $B(u,v,w)$ is the Fourier Transform (FT) of $b(x,y,z)$, $F(u,v,w)$ is the FT of $f(x,y,z)$ and $H(u,v,w)$ is the FT of $h(x,y,z)$.

Due to the circular aperture of the microscope, the transfer function (TF), which is the normalized $H(u,v,w)$, is zero-valued for most of the frequencies in the Fourier domain [6]. In the region where the TF has non-zero values it works as a low pass filter and in the regions where it has zero values it removes the image content in that region. Now, in COSM images, the predominant noise is a signal-dependent one that can be modeled by a Poisson distribution. The noise can be incorporated into the model by considering the observation $b(x,y,z)$ as an inhomogeneous Poisson process $g(x,y,z)$. Of course, there are several other sources of noise in COSM, including additive, and signal independent, but in this work we are only concerned with the Poisson one.

Then, the problem is to find an estimate of the true specimen given the blurred and noisy observed image. It is well known that this problem is ill posed and several algorithms have been proposed to solve it [7 -10]. In order to improve the resolution, the contrast, and also recover the missing frequencies, we propose the use of the POCS methodology. POCS is a powerful mathematical tool proposed by Bregman [11] and Gubin et al. [12] and later introduced in the signal and image processing literature by Youla [13]. The POCS method has the advantage of incorporating into the problem formulation *a priori* knowledge in the form of convex constraints. Some attempts were already made using POCS for deconvolution of 3D microscopic images [14 - 16] but these methods consider noise to be stationary, white Gaussian and also do not address the problem of the super-resolution (recover the missing frequencies). In order to address these problems using the projection theory we propose the use of three sets of *a priori* information. The first set ($S_1$) is to perform the deconvolution of the blurred image with the PSF of the microscope, the second set ($S_2$) is based on the hypothesis that the images have finite extent in all directions in order to recover the missing cone of frequencies and the last set ($S_3$) is to ensure the positiveness of the solution. Using these three sets the method demonstrates good performance in terms of the restoration results and also of the convergence rate.

## Materials and Methods

Projection onto Convex Sets is an important result from vector-space projections theory [17–19]. Formally, it looks for a solution satisfying some *a priori* information about the problem. Such information is incorporated into the problem formulation in the form of convex sets (convex constraints). Given a set S and any points $x_1$ and $x_2$ that belong to $S$, then $S$ is convex if $x = \mu \cdot x_1 + (1-\mu) \cdot x_2$ also belongs to $S$ and $0 \le \mu \le 1$. For the sake of simpler notation, in the discussion below we can consider only cubic images with size $N$ x $N$ x $N$ into a 3D Euclidean space and write Eq. (1) in vector-matrix notation as

$$\mathbf{g} = \mathbf{H} \cdot \mathbf{f} \quad (3)$$

where $\mathbf{g}$ and $\mathbf{f}$ are $N^3 x 1$ vectors that are formed by stacking the elements of $g(x,y,z)$ and $f(x,y,z)$ respectively. Matrix $\mathbf{H}$ is the $N^3 x N^3$ blurring matrix that gives the blurring degradation effects where the elements are samples $h(x,y,z)$. We observe again that $g(x,y,z)$ is the version of $b(x,y,z)$ degraded by Poisson noise.

Now, let $S_1$, $S_2$, ..., $S_M$ be $M$ closed and convex sets where $S_k \subset H$, $H$ is a Hilbert space and $\varnothing \neq S = \bigcap_{k=1}^{M} S_k$. In our case $H$ is the space $L^2$ of square-integrable functions. For each set $S_k$ we define a projection operator $P_k$ such that for each function $\mathbf{f} \prod \mathrm{H}$ we have

$$\|\mathbf{f} - \mathbf{P}_k \cdot \mathbf{f}\| \le \|\mathbf{f} - \mathbf{g}\| \quad (4)$$

over all $\mathbf{g} \prod S_k$. Hence, $\mathbf{P_k} \cdot \mathbf{f}$ is the nearest element of $\mathbf{f}$ in $S_k$ and if $S_k$ is *closed* and *convex* $\mathbf{P}_k \cdot \mathbf{f}$ is unique. For an arbitrary starting point $\mathbf{f}^{(0)}$ the recursive relation in Eq. (5) generates a sequence $\{\mathbf{f}^{(n)}\}$ and it can be shown that iterates will converge weakly to a point of $S$.

$$\mathbf{f}^{(n+1)} = \mathbf{P}_M \cdot \mathbf{P}_{M-1} \cdot \mathbf{P}_1 \cdot \mathbf{f}^{(n)} \quad (5)$$

The recursive relation (5) is the well-known cyclic POCS algorithm. In its relaxed version it has the form

$$\mathbf{f}^{(n+1)} = \mathbf{T}_M \cdot \mathbf{T}_{M-1} \cdot \mathbf{T}_1 \cdot \mathbf{f}^{(n)} \quad (6)$$

where $\mathbf{T}_k$ is defined by $\mathbf{T}_k = \mathbf{I} + \lambda_{n,k} \cdot (\mathbf{P}_k - \mathbf{I})$ for the relaxation parameter $\lambda_{n,k} \in (0,2)$. In the general case, this parameter depends on the projector and on the interaction step, as well.

Sets presented in this work are closed and convex and they also have a non-empty intersection, but in the general case this methodology has an extension for the case where the sets are not convex and do not intersect themselves. We refer the reader to references [17-19] for a more complete discussion of these cases.

In order to perform the 3D deconvolution and also to take into account the nature of the Poisson noise into COSM images, we propose the use of a prototype constraint [20] based on the Goodman and Belsher's filter [21] to construct the first set. It is a linear, space-invariant, minimum mean square restoration filter for the Poisson image noise model using the orthogonality principle in the Fourier domain. It was first derived by Goodman and Belsher [21] and later used by Lo [22] for 2D images with Poisson noise. In this paper we extend the filter for the 3D case. The filter in the 3D case is given by

$$GB(u,v,w) = \frac{\overline{H}(u,v,w)}{\left|H(u,v,w)\right|^2 + \frac{1}{\gamma}} \tag{7}$$

where $\gamma = \overline{N} \cdot P_f(u,v,w)$, $\overline{N}$ is the ensemble mean number of photon counts and $P_f(u,v,w)$ is the power spectrum density of the true object. Eq. (6) is used to build the first set $S_1$ in the form of a prototype constraint [20]. The set is then given by

$$S_1 = \left\{ \mathbf{y} : \left\| \mathbf{p} - \mathbf{y} \right\|^2 \le \xi \right\} \tag{8}$$

where **p** represents the prototype image, **y** represents an arbitrary member of the set $S_1$ and $\Rightarrow$ represents the bounded variation between **p** and **y**. The prototype image **p** is created applying the Goodman-Belsher filter on the blurred and noisy observed image. Because it is a pointwise filter in the Fourier domain we can define the correspondent set into the frequency domain by

$$S_1 = \left\{ \mathbf{y} : \left\| \mathbf{P} - \mathbf{Y} \right\|^2 \le \xi \right\} \tag{9}$$

where **P** and **Y** are the discrete Fourier transform (DFT) of **p** and **y**, respectively. For a particular triple of frequencies *(u,v,w)* the projection for an arbitrary function *y(x,y,z)* onto $S_1$ is given by

$$\mathbf{y}^* = \mathbf{P}_1 \cdot \mathbf{y} \Leftrightarrow$$

$$Y^*(u,v,w) = \begin{cases} P(u,v,w) - \sqrt{\xi(u,v,w)} \cdot \dfrac{\Delta(u,v,w)}{\left|\Delta(u,v,w)\right|} & \text{if} \\ & \left|\Delta(u,v,w)\right|^2 \ge \xi(u,v,w) \\ Y(u,v,w) & \text{otherwise} \end{cases} \tag{10}$$

where $\Delta(u,v,w) = P(u,v,w) - Y(u,v,w)$ and the vector $\Rightarrow$ is constructed as

$$\xi = c \cdot E\left\{ \left\| \mathbf{p} - \mathbf{f} \right\|^2 \right\} \tag{11}$$

which is the expected variation when the true solution is known. The user chooses the constant c and it is determined by the confidence that we have about the constraint.

The second set intends to recover some of the missing frequencies lost due to the TF. The problem to recover the lost frequencies is called super-resolution and it can be achieved by imposing additional information over the problem [23]. In this sense, we can use the *a priori* knowledge about the region of support of the object as a constraint to the recovery process. We refer the reader to the paper of Hunt [23] to interesting considerations about super-resolution.

Then, the set $S_2$ is the set of all functions of finite extent in the three directions and is defined by

$$S_2 = \left\{ \mathbf{y} : y(x,y,z) = 0 \quad \textit{for all } (x,y,z) \notin S_f \right\} \tag{12}$$

where $S_f$ is the support of the true object $f(x,y,z)$. The projector for this set is given by

$$P_2 \cdot \mathbf{y} = \begin{cases} y(x,y,z) & \textit{if } (x,y,z) \in S_f \\ 0 & \textit{otherwise} \end{cases} \tag{13}$$

The last set imposes positiveness of the solution since image intensity is always non-negative. We observe that the positiveness constraint can also be viewed as a way to achieve super-resolution because it is another source of non-linearity that extends information below the diffraction limit above the diffraction limit. The set is defined by

$$S_3 = \left\{ \mathbf{y} : y(x,y,z) \ge 0 \quad \textit{for all } (x,y,z) \in S_f \right\} \tag{14}$$

and the projector is given by

$$P_3 \cdot \mathbf{y} = \begin{cases} y(x,y,z) & \textit{if } y(x,y,z) \ge 0 \\ 0 & \textit{otherwise} \end{cases} \tag{15}$$

Then, given a starting image $\mathbf{f}^{(0)}$ (for instance, the blurred and noisy observed image) and the three sets described above, we define the POCS algorithm for 3D deconvolution of microscopic biological images as

$$\mathbf{f}^{(n+1)} = \mathbf{P}_3 \cdot \mathbf{P}_2 \cdot \mathbf{P}_1 \cdot \mathbf{f}^{(n)} \tag{16}$$

## Results

We have implemented the algorithm of Eq. (5) in a UNIX environment using C++ language. In the implementation of Eq. (7) we used the periodogram technique for the power spectrum density estimate of the true image. However, it is well known that the periodogram is a biased estimate of the power spectrum and we expect that the results could be further improved by using more accurate techniques of estimation. The mean number of photon counts $\overline{N}$ was estimated under a uniform 3x3x3 volumetric window over the observed image. In Eq. (11) we assume c = 1 for the confidence interval for all results, which implies 50% of confidence in the case of distributions that are symmetric about their mean. The fast Fourier transform algorithm is adopted henceforth.

We have tested the algorithm with synthetic images (phantoms) and also with polystyrene bead images. A test phantom consists of a 64x64x64 pixels image with several square structures which extends through all three dimensions and has sharp edges. Figure 1 shows two sections of the phantom. Figure 2 shows the corresponding sections of the phantom degraded by a theoretical PSF and also by a signal-dependent Poisson

noise. We have used the Washington University's XCOSM software [6] in order to calculate the theoretical PSF and also to simulate a standard non-confocal (wide-field) microscope with a 100X objective lens, a numerical aperture of 1.3, a refractive index of the lens immersion oil of 1.515 and an emission wavelength of 530 nm.

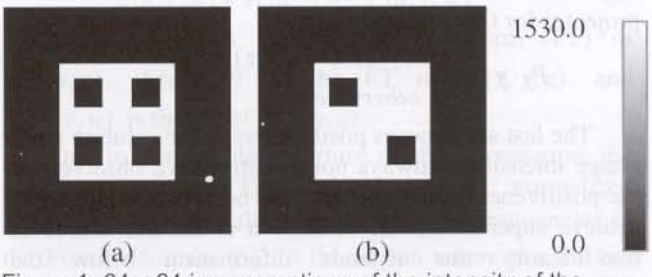


Figure 1: 64 x 64 image sections of the intensity of the phantom: (a) slice 23; (b) slice 39. The voxel size is 0.1426 x 0.1426 x 0.1426 microns.

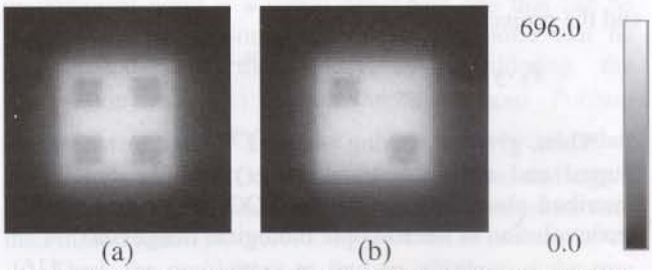


Figure 2: Sections through the simulated microscopic data and degraded by Poisson signal-dependent noise. In order to simulate a standard non-confocal microscope, the theoretical point spread function (PSF) was calculated using the Washington University XCOSM software, where the PSF corresponds to a 100X objective lens with a numerical aperture of 1.3.

Figure 3 shows the sections of the recovered phantom image using the cyclic POCS method of Eq. (16) with the three sets above. The method converged in only 18 interations.

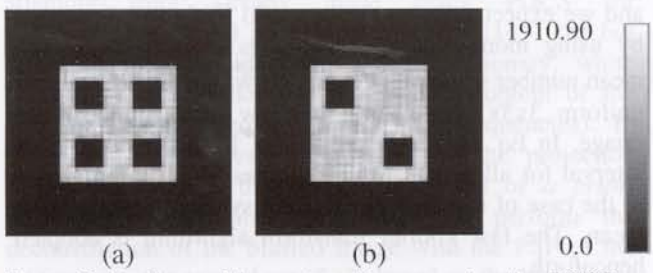


Figure 3: Sections of the restored image using the POCS method of Eq. (16). The improvement in SNR of the restored image is 12.59 dB. The POCS algorithm converged in 18 iterations.

From Figure 3 we observe that the algorithm was able to remove most of the blurring and also improve the contrast into the phantom image.

There exist in the literature several figures of merit to quantify the results of the restoration. We have chosen the improvement in signal to noise ratio to check the amount of restoration of our method. The improvement in signal-to-noise ratio (ISNR) in decibels (dB) is defined by

$$ISNR = 10 \cdot \log_{10} \frac{\sum_{j=1}^{N^3} (f_j - g_j)^2}{\sum_{j=1}^{N^3} (f_j - \hat{f}_j)^2} \qquad (17)$$

where $f_j$ is the $j$th element of the phantom image $\mathbf{f}$, in vector-matrix notation, $\hat{f}_j$ is the $j$th element of the restored image $\hat{\mathbf{f}}$ and $\hat{g}_j$ is the $j$th element of the degraded phantom image $\mathbf{g}$. The ISNR for the phantom in Figure 3 was 12.59 dB.

In order to check the super-resolution capability of the method we have applied the algorithm for the image in Figure 2 using only the sets $S_1$, and $S_3$. Figure 4 shows the restored sections in this case where the algorithm converged in 27 interactions and the ISNR was 9.49 dB.

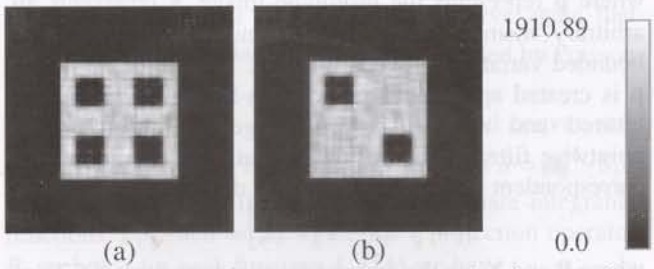


Figure 4: Sections of the restored image using the sets $S_1$ and $S_3$. The improvement in SNR of the restored image is 9.49 dB. The POCS algorithm converged in 27 iterations.

We observe that the shapes of the structures in the Figure 3 are sharper than the shapes in Figure 4. Figure 5a shows a section of the 3D FT of the recovered image from Figure 3 and Figure 5b shows a section of the 3D FT of the recovered image from Figure 4.

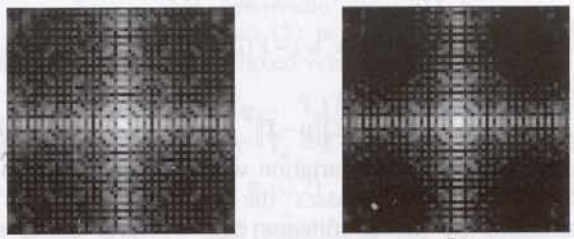


Figure 5: (a) 3D Fourier transform of the restored image using the sets $S_1$, $S_2$ and $S_3$; (b) 3D Fourier transform of the restored image using the sets $S_1$ and $S_3$.

We see that the use of the sets $S_1$, $S_2$ and $S_3$ in Eq. (16) is able to recover more frequencies than the use of only

the sets $S_1$ and $S_3$ as one can see comparing the Fourier spectrum in Figure 5a and Figure 5b.

Figure 6a and 7a show sections of a spherical bead image with 15 ⇐m of diameter. The image was acquired using a wide-field microscope with a 60X objective lens, a numerical aperture of 1.4, a refractive index of the lens immersion oil of 1.515 and an emission wavelength of 630 nm (red) in Figure 6 and 530 nm (green) in Figure 7.

Figure 6b and 7b show the sections of the restored *bead* images using Eq. (16).

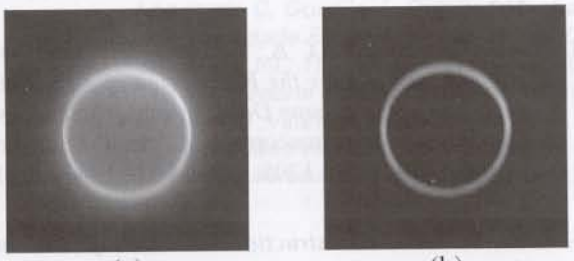

(a) (b)

Figure 6: (a) Original *bead* image with emission wavelength of 630 nm; (b) Restored image.

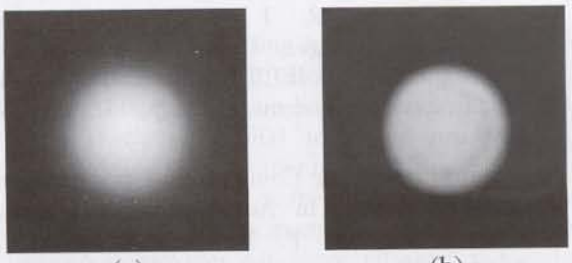

(a) (b)

Figure 7: (a) Original *bead* image with emission wavelength of 530 nm; (b) Restored image.

Figure 8 shows an example of a blurred and noisy real 3D image and Figure 9 shows the corresponding recovered image.

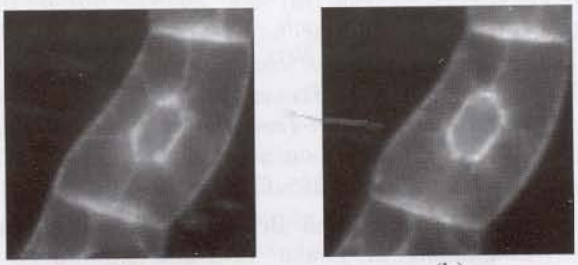

(a) (b)

Figure 8: Sections of the 128x128x128 blurred image of an endoplasmic reticulum cell. The image was acquired using a fluorescence microscope with a 20X 0.75NA lens. (a) slice 65; (b) slice 75.

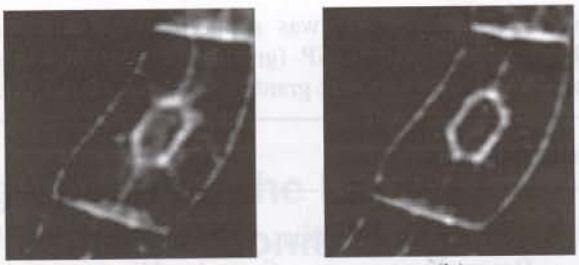

(a) (b)

Figure 9: Sections of the restored endoplasmic reticulum image.

## Discussion

We have used a cyclic POCS method for 3D deconvolution of biological microscopic images. From the results one can note that this methodology presents a fast convergence using the three sets above and it was able to remove most of the blurring of the degraded images as one can see from the ISNR measurements. Also, the method presented a good visual performance for real 3D biological images. We have tested the method for different levels of Poisson noise and we can verify the robustness of the algorithm for highly noise images. Also, analyzing the FT of the restored images (Figure 5) we conclude that the method is able to achieve super-resolution.

Furthermore, it had a fast convergence and it demonstrated a good performance in terms of both visual results and cost-benefit analysis for all the studied images. However, we can further improve the convergence rate of the POCS algorithm using other approaches for the set theoretic image recovery problem. For instance, Combettes [17] has proposed an extrapolated parallel projection method that out performs the convergence rate for the POCS method where the relaxation parameter into Eq. (6) extrapolates the interval (0,2). Further, we are working to incorporate into the method other constraints as, for instance, to reduce regularization artifacts generated by minimum mean square filters as Wiener and Goodman and Belsher's filters and also to consider other kinds of noise as the additive, signal independent one that cames from the CCD camera.

We conclude that the POCS method can be a powerful tool to be applied in optical-sectioning microscopy.

## Acknowledgments

The authors would like to thank Prof. Chrysanthe Preza and Prof. Donald L. Snyder from ESSRL of the Electrical Engineering Department and Prof. Barbara Pickard from the Biology Department, both from Washington University in St. Louis, USA, for offering the facilities of their laboratories and also for their helpful

discussions. This work was supported by a Brazilian scholarship from FAPESP (grant number 99/01351-2), and by a FINEP-RECOPE grant number 77.97.0575.00.

## References


1. Swedlow, J. R.; Sedat, J. W.; Agard, D. A. *Deconvolution in Optical Microscopy*. In Deconvolution of Images and Spectra, P. A. Jansson, Ed., Second Edition. Academic Press, New York, pp. 284-309, 1997.
2. Combettes, P. L. *The Foundations of Set Theoretic Estimation*. Proceedings of the IEEE, Vol. 81, No. 2, pp. 182-208, February 1993.
3. Costa, L. da F. and Velte, T. J. *Automatic Characterization and Classification of Glangion Cells from the Salamander Retina*. The Journal of Comparative Neurology, Vol. 404, pp. 33-51, 1999.
4. Agard, D. A. *Optical Sectioning Microscopy: Cellular Architecture in Three Dimensions*. Ann. Rev. Biophys. Bioeng, Vol. 13, pp. 191-219, 1984.
5. Weinstein, M. and Castleman, K. R. *Reconstructing 3D Specimens from 2D Section Images*. In Quantitative Imagery in the Biomedical Sciences I, R. E. Herron, Ed., Proc. of the SPIE, Vol. 26, pp. 131-138, 1971.
6. McNally, J. G.; Conchello, J. A.; Rosenberger, F. U.; Preza, C.; Markhan, J. *Tutorial-Image Restoration for 3-D Microscopy*. April 26-27, IBC, Washington University, St. Louis, MO, 1996.
7. Preza, C.; Miller, M.I.; Conchello, J.A. Image *Reconstruction for 3-D Light Microscopy with a Regularized Linear Method Incorporating a Smoothness Prior*, IS&T/SPIE Proc., R.S. Acharya & D.B. Goldgof, Eds., pp. 129-139, 1992.
8. Preza, C.; Miller, M. I.; Thomas, L. J. ;McNally, J. G. *Regularized Linear Method for Reconstruction of Three-Dimensional Microscopic Objects from Optical Sections*. J. Opt. Soc. Am. A., Vol. 9, No.2, pp. 219-228, February 1992.
9. Conchello, J. A. *Super-Resolution and Convergence Properties of the Expectation-Maximization Algorithm for Maximum-Likelihood Deconvolution of Incoherent Images*, J. Opt. Soc. Am. A, Vol. 15, No.10, pp. 2609-2620, October 1998.
10. Conchello, J. A. and McNally, J. G. *Fast Regularization Technique for Expectation Maximization Algorithm for Computational Optical Sectioning Microscopy*. In Three-Dimensional Microscopy: Image Acquisition and Processing, C. J. Cogswell, G. S. Kino & T. Wilson, Eds., SPIE 2655, pp.199-208, 1996.
11. Bregman, L. M. *Finding the Common Point of Convex Sets by the Method of Successive Projections*. Akud. Nauk USSR, Vol. 162, pp.487 - 490, 1965.
12. Gubin, L. G., Polyak, B. T. and Raik, E. V. *The Method of Projections for Finding a Common Point of Convex Sets*. USSR Computational Maths. And Mathematical Phys., Vol. 7, pp. 1-24, 1967.
13. Youla, D. C. *Generalized Image Restoration by the Method of Alternating Orthogonal Projections*. IEEE Trans. On Circuits Syst., CAS 25, pp.695-702, 1978.
14. Koshy, M; Agard, D. A.; Sedat, J. W. *Solution of Toeplitz Systems for the Restoration of 3-D Optical Sectioning Microscopy Data*. Bioimaging and Two-Dimensional Spectroscopy, L. C. Smith, Ed., Proc. of the SPIE, Vol. 1205, pp. 64-71, Los Angeles, 1990.
15. Lenz, R. 3-D *Reconstruction with a Projection onto Convex Sets Algorithm*. Optics Communications, Vol. 57, No 1, pp. 21-25, 1986.
16. Gopalakrishman, V. K.; Ramachandran, R. P.; Wilder, J.; Mammone, R. J. *Restoration of Three Dimensional Images Using the Row Action Projection Method*. IEEE International Symposium on Circuits and Systems, Orlando, FL, pp. 33-36, 1999.
17. Combettes, P. L. *The Convex Feasibility Problem in Image Recovery*. In Advances in Imaging and Electron Physics, P. Hawkes, Ed., Vol. 95, Academic Press, New York, pp. 155-270, 1996.
18. Combettes, P. L. *Convex Set Theoretic Image Recovery: History, Current Status, and New Directions*. Journal of Visual Communications an Image Representation. Vol. 3, No 4, December, pp. 307-315. 1992.
19. Stark, H. and Yang, Y. *Vector Space Projections, A Numerical Approach to Signal and Image Processing, Neural Nets, and Optics*. Wiley, 1998.
20. Sezan, M. and Trussell. J. *Prototype Image Constraints for Set-Theoretic Image Restoration*. IEEE Transactions on Signal Processing, Vol. 39, No. 10, pp. 2275-2285, October 1991.
21. Goodman, J. W. and Belsher, J. F. *Fundamental Limitations in Linear Invariant Restoration of Atmospherically Degraded Images*. Proc. SPIE 75, pp. 141-154, 1976.
22. Lo, C. M. *Estimation of Image Signals with Poisson Noise*. University of Southern California. Doctoral Thesis, 1979.
23. Hunt, B. R. *Super-Resolution of Images: Algorithms, Principles, Performance*. International Journal of Imaging systems and Technology, Vol. 6, pp. 297-304, 1995.